

ROOM-TEMPERATURE FORMATION OF HIERARCHICAL NANOARCHITECTURES ON ZNO NANOWIRES FOR SOLAR CELLS

Wei-Ting Jiang, Chun-Te Wu and Jih-Jen Wu*

Department of Chemical Engineering, National Cheng Kung University, Tainan 701, Taiwan

Introduction

ZnO nanostructures have attracted considerable attention for dye-sensitized solar cell (DSSC) applications because of its low crystallization temperature, anisotropic growth behavior and superior electron transport properties.¹ In comparison with the conventional TiO₂ nanoparticle (NP) anode of DSSC, in which electron transport *via* trapping/detrapping mechanism, superior electron transport properties have been demonstrated in ZnO-based DSSCs with various anode structures, such as single-crystalline nanowire (NW),^{2,3} porous crystalline film,⁴ NW/NP composite film,^{5,6} and nanodendrite/NP composite film.⁷

Recently, we have demonstrated a novel ZnO nanocactus (NC) array for use in DSSCs.⁸ A room-temperature (RT) chemical bath deposition (CBD) was developed to construct hierarchical nanostructures on ZnO NWs for the formation of ZnO NC arrays. The hierarchical ZnO nanostructures on NWs provide not only larger and more fitting surface for dye adsorption but also faster electron transport pathways compared to the as-prepared ZnO NW anode, resulting in a significant enhancement of the performance of ZnO NW DSSC. With an anode thickness of 3.3 μm , a DSSC efficiency of 3.32% is achieved.⁸ In the presentation, construction of other ZnO nanoarchitectures by applying the RT CBD on ZnO NW arrays, including long ZnO NC and ZnO nanosheet (NS)/NW composite arrays for use in DSSCs will be reported.

Experimental

Aligned ZnO NW arrays were first grown on the seeded FTO substrates by CBD in a 0.02M aqueous solution of zinc acetate ($\text{Zn}(\text{CH}_3\text{COO})_2 \cdot 2\text{H}_2\text{O}$, ZnAc \cdot 2H₂O, Merk, 99.5 %) and hexamethylenetetramine ($\text{C}_6\text{H}_{12}\text{N}_4$, HMTA, Riedel-de Haen, 99.5 %) at 95 °C.⁵⁻⁸ A 3- μm NW array is obtained after a 3h CBD. The density of the ZnO NWs is adjustable by the seed layer. ZnO NW arrays with longer thickness are achievable by multiple-batch deposition. For construction of the hierarchical nanostructures on ZnO NWs, the ZnO NW array/FTO substrate was subsequently immersed in a stirred aqueous solution of ZnAc \cdot 2H₂O and NaOH at RT. The limpid solution was obtained by preparing a solution of 0.57 M ZnAc \cdot 2H₂O and 5 M NaOH and then further diluting by a factor of 8-12.

Dye adsorption was carried out by immersing the anode in a 5×10^{-4} M acetonitrile/*t*-butanol (1:1) solution of D149 at RT for 1h. The sensitized electrode and platinized FTO counter electrode were sandwiched together with 25- μm -thick hot-melt spacers (SX 1170-25, Solaronix SA). Liquid electrolyte solutions composed of 0.5 M Pr₄NI and 50 mM I₂ in a 1:4 volume ratio of ethylene carbonate and acetonitrile was employed for the D149-sensitized DSSCs. Photovoltaic properties of the DSSCs were measured under AM 1.5 simulated sunlight at 100 mWcm⁻² (300 W, Model 91160A, Oriol).

Results and Discussion

An aligned ZnO NW array, with a thickness of 10 μm and a density of $\sim 1 \times 10^9 \text{ cm}^{-2}$, is grown on the seeded FTO substrate using multiple-batch CBD. ZnO NC array is then formed via the RT CBD. Top-view and cross sectional-view SEM images of the ZnO NC array

are illustrated in Figures 1(a) as well (b) and (c), respectively. As shown in Figure 1, the hierarchical nanostructures of spines on the ZnO NWs are successfully synthesized at RT without any assistance of seeds and organic structure-directing agents. In addition, Figure 1(c) reveals that the spines are parallel with each other on ZnO NW surface with a specific angle of $\sim 110^\circ$ to the NWs. TEM characterization indicates that the same as the primary NW, the spine is single crystalline and grows along [0001].⁸

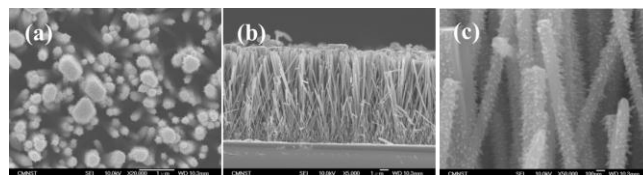


Figure 1. (a) Top-view and (b), (c) cross sectional-view SEM images of the ZnO NC array.

Current density (*J*)-voltage (*V*) characteristic of the D149-sensitized ZnO NC DSSC with an anode thickness of 10 μm is shown in Figure 2. Short-circuit current density (*J*_{sc}), open-circuit voltage (*V*_{oc}) and fill factor (*FF*) of the ZnO NC DSSC are 10.69 mA cm⁻², 0.71 V and 0.71, respectively. An efficiency of 5.37% is achieved simply by the formation of the RT hierarchical nanostructures on the ZnO NW array.

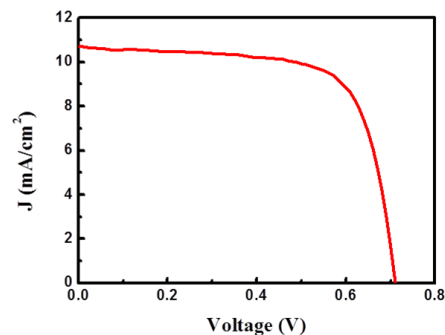


Figure 2. *J*-*V* characteristic of the D149-sensitized ZnO NC DSSC with an anode thickness of 10 μm .

In addition to the NC array, ZnO NS/NW composite array is also successfully formed by applying the RT CBD on the 2.7- μm -thick ZnO NW array. Top-view and cross sectional-view SEM images of the ZnO NS/NW composite array are shown in Figures 3(a) and (b), respectively. It reveals that ZnO NSs are constructed on the top and within the interstices of ZnO NW array after the RT CBD. The thickness of the NSs on the top is $\sim 0.3 \mu\text{m}$. TEM characterization shows that the NS possesses a single-crystalline structure and growth direction is along [0001] as well.

The D149-sensitized ZnO NS/NW composite array is employed to be the photoanode of DSSC. With an anode thickness of 3 μm , the D149-sensitized ZnO NS/NW DSSC demonstrates the efficiency over 4%. The diffuse reflection spectra of the ZnO NS/NW and NW arrays indicate the light scattering ability of the ZnO NSs in the ZnO NS/NW composite array. IPCE spectrum of the D149-sensitized ZnO NS/NW DSSC shows a wider response range in the long wavelength compared to that of the D149-sensitized ZnO NW DSSC, confirming the light scattering ability of the NSs in the ZnO NS/NW DSSC.

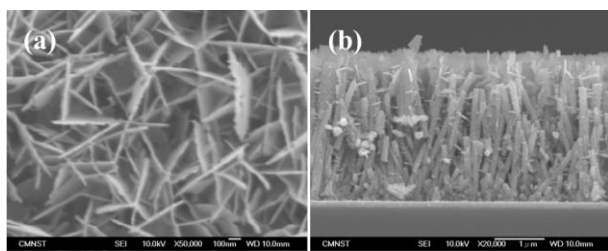


Figure 3. (a) Top-view and (b) cross sectional-view SEM images of the ZnO NS/NW composite array.

Conclusions

ZnO nanoarchitectures, including ZnO NC arrays and ZnO NS/NW composite arrays, have been constructed on FTO substrates by applying the RT routes on ZnO NW arrays. The same as the ZnO NW, the spine and sheet in the hierarchical ZnO NC and NS/NW composite arrays possess single crystalline structure. With an anode thickness of 10 μm , an efficiency of 5.37% is achieved in the D149-sensitized ZnO NC DSSC. Moreover, with an anode thickness of 3 μm , the D149-sensitized ZnO NS/NW DSSC demonstrates the efficiency over 4%. The diffuse reflection and IPCE spectra show the light scattering ability of the ZnO NSs in the ZnO NS/NW composite anode. The results indicate that the efficiency of the ZnO NW DSSC is significantly enhanced simply by the formation of the RT hierarchical nanostructures on the ZnO NW array.

Acknowledgement. Financial supports from the National Science Council and the Bureau of Energy, Ministry of Economic Affairs in Taiwan under Contract No. NSC 99-2221-E-006-198-MY3 and 100-D0204-2, respectively, are gratefully acknowledged.

References

References should use ACS style. References may be inserted and numbered manually, or automatically by using the endnote/footnote function of the word processor. For manual insertion, format the references as follows:

- (1) Zhang, Q.; Dandeneau, C. S.; Zhou, X.; Cao, G. *Adv. Mater.* **2009**, *21*, 4087.
- (2) Law, M.; Greene, L. E.; Johnson, J. C.; Saykally, R.; Yang, P. D. *Nat. Mater.* **2005**, *4*, 455.
- (3) Galoppini, E.; Rochford, J.; Chen, H. H.; Saraf, G.; Lu, Y. C.; Hagfeldt, A.; Boschloo, G. *J. Phys. Chem. B* **2006**, *110*, 16159.
- (4) Yoshida, T.; Zhang, J.; Komatsu, D.; Sawatani, S.; Minoura, H.; Pauporte, T.; Lincot, D.; Oekermann, T.; Schlettwein, D.; Tada, H.; Wohrle, D.; Funabiki, K.; Matsui, M.; Miura, H.; Yanagi, H. *Adv. Funct. Mater.* **2008**, *18*, 1.
- (5) Ku, C.-H.; Wu, J.-J. *Appl. Phys. Lett.* **2007**, *91*, 093117.
- (6) Wong, D. K.-P.; Ku, C.-H.; Chen, Y.-R.; Chen, G.-R.; Wu, J.-J. *ChemPhysChem* **2009**, *10*, 2698.
- (7) Wu, C.-T.; Liao, W.-P.; Wu, J.-J. *J. Mater. Chem.* **2011**, *21*, 2871.
- (8) Wu, C.-T.; Wu, J.-J. *J. Mater. Chem.* **2011**, *21*, 13605.